Elucidating the performance limits of perovskite nanocrystal light emitting diodes

Thomas Morgenstern,[*,†] Carola Lampe,[‡] Tassilo Naujoks,[†] Matthew Jurow,[¶] Yi Liu,[¶] Alexander S. Urban,[‡] and Wolfgang Brütting[*,†]

[†]*Institute of Physics, University of Augsburg, 86135 Augsburg, Germany*

[‡]*Nanospectroscopy Group, Nano-Institute Munich, Department of Physics,*
Ludwig-Maximilians-Universität München, 80539 Munich, Germany

[¶]*Molecular Foundry, Lawrence Berkeley National Laboratory, Berkeley, California 94720,*
United States

E-mail: Thomas.morgenstern@physik.uni-augsburg.de; bruetting@physik.uni-augsburg.de

Abstract

The unique optical properties of lead halide perovskites have drawn significant attention towards their application in light emitting devices (LEDs) in recent years. While quantum yield, emission wavelength and stability are already in the focus of many research groups, the orientation of the emissive transition dipole moments (TDM) has rarely been investigated. As known from other thin film applications such as organic LEDs, this quantity can severely affect the light outcoupling of the device and thereby limit the external quantum efficiency. In this work, we investigate $CsPbBr_3$ nanoplatelets of variable thickness and determine the orientation of their TDMs from thin film radiation pattern analysis. We then apply optical simulations to elucidate the performance limits of perovskite based blue LEDs in prototypical device architectures. We find that with increasingly beneficial horizontal orientation, the maximum efficiency

achievable increases to values close to 30%. However, since the photoluminescence quantum efficiency degrades considerably for decreasing thickness, the overall device efficiency does not significantly improve. Thus, for the currently available material sets we can conclude that while for nanocubes the non-ideal orientation limits device performance, devices with nanoplatelets are limited by non-optimal photoluminescence quantum yields.

Keywords

Perovskite nanocrystal LED, transition dipole alignment, performance limit, light outcoupling

1   Introduction

Lead halide perovskites (LHPs) have recently gained considerable attention for applications in thin-film optoelectronic devices. The family of hybrid organic-inorganic LHPs, the most renowned being methylammonium lead iodide (MAPI), has revolutionized the field of thin-film photovoltaics in less than ten years.[1–3] Recently, however, they have also generated increasing attention in the context of light emission. Particularly LHP nanocrystals (NCs) are attractive as luminescent materials for light-emitting diodes (LEDs). Combining the advantages of bulk LHPs – notably their defect tolerance, solution processability, and electronic bandgap tunability – with well-known features of colloidal quantum dots (QDs), such as high photoluminescence quantum yield (PLQY) with narrow emission linewidths, as well as size- and composition-tunable colours.[4–6] Owing to their high PLQY, LHP NCs are meanwhile used in display applications, where they typically function as optical down converters. Excited by the light of a blue or UV-emitting LED, they produce light between the green and near infrared (NIR) parts of the optical spectrum, covering a large colour gamut. In this arena they compete with conventional semiconductor QDs and might even outperform

InP as an alternative Cd-free emitter system.

In contrast to these optically pumped systems, **electroluminescence** (EL), i.e., the direct electrical excitation of LHP light emitters, has been demonstrated only recently. The first electroluminescent green and red perovskite LEDs (PeLEDs) were reported in 2014 by Tan et al., reaching external quantum efficiencies (EQEs) of 0.1 % and 0.23 %, respectively.[7] Until now, extensive research is going on, improving EQEs of perovskite LEDs up to around 20 % EQE.[8–11] While green and red emitters are well-examined blue emitting PeLEDs are still lagging behind with an EQE of approximately 2 %.[12] Reasons for that are low PLQY for Cl-containing NCs and difficulties in the injection of electrons and holes into conduction and valence band.[13–17] Recently Bohn et al. showed a synthesis routine for all-inorganic LHP nanoplatelets (NPls) with high PLQY and narrow, tunable emission between 435 nm and 497 nm. Herein, different emission wavelengths can be achieved by monolayer-precise tuning of the thickness of $CsPbBr_3$ NPls taking advantage of strong quantum confinement.[18] Especially blue emission with a dominant wavelength of less than 475 nm is of great interest since it is necessary to meet the requirements for the BT2020 television standard.[19]

Concerning the application of LHP NCs in electroluminescent devices, a fundamental understanding of the factors determining their efficiency is required. In particular, the problem of light extraction in PeLEDs is of paramount importance.[20] Specifically, the direction of the transition dipole moment (TDM), which has been found to be a very powerful tool in organic LEDs, has not been investigated yet in detail in LHP systems. Consequently, many devices lack a clear evaluation of their theoretical performance limit given by the optical properties of the emissive layer stack.

2 Results and discussion

2.1 Optical simulations

In general, the overall performance of a thin film LED is given analogously to a formalism proposed for OLEDs.[15,21] Accordingly, the external quantum efficiency η_{EQE} can be expressed as:

$$\eta_{\text{EQE}} = \gamma \cdot q_{\text{eff}} \cdot \eta_{\text{out}} \tag{1}$$

Herein, γ denotes the charge carrier balance, so the ratio of electrons and holes in the emission layer (EML) that recombine. This parameter is critical, especially for blue emitting perovskites, and is typically controlled through the device architecture.[15,18] As this paramter has been investigated in previous publications, we will not further address this factor here and assume it to be unity. The remaining factors limiting the performance are thus the effective radiative quantum yield (q_{eff}) and the light outcoupling efficiency (η_{out}). Whether or not an additional, fourth factor for the spin of the excited state has to considered in PeLEDs is currently under debate.[22,23] The q_{eff} takes into account the material specific intrinsic quantum yield (q) – with the PLQY being a good approximation for it – and the coupling of the excited states to the photon field within the microresonator of an LED – also known as the Purcell effect. The PLQY can be measured directly for a given material by use of an integrating sphere. However, both the outcoupling efficiency and the Purcell factor need to be derived from numerical simulations. Therein, the optical properties of the system such as film thicknesses and refractive indices of the individual layers are important input parameters.

Another key factor determining the outcoupling efficiency is the radiation pattern of the emissive species. This property is affected both by the orientation of the emissive transition dipole moments (TDM) of the nanocrystals, as indicated in Fig. 1a, and by the refractive index of the emissive layer. With both having a comparable effect on η_{out}, it makes sense to

introduce a figure of merit which takes both contributions into account. One such parameter is the dimensionless alignment constant (ζ), which quantifies the angular distribution of emitted power, and is given by the refractive index n_{EML} and the angle of the emissive TDM (φ_{TDM}) with respect to the film surface via:[24]

$$\zeta = \frac{\sin^2 \varphi_{\text{TDM}}}{n_{\text{EML}}^4 - \sin^2 \varphi_{\text{TDM}} \left(n_{\text{EML}}^4 - 1\right)} \tag{2}$$

This parameter can take values between 0 (corresponding to perfectly horizontal TDMs) and 1 (corresponding to perfectly vertical TDMs) and consequently is desired to be as low as possible to enhance the radiative outcoupling of emitted light out of the stack. This can be achieved by reducing the angle of the TDM (φ_{TDM}) or by increasing the refractive index (n_{EML}) of the EML. To investigate how these parameters would affect a state-of-the-art perovskite LED and obtain performance limits, we performed optical simulations following an approach widely used for OLEDs and assuming the LHP NCs as emitting classical dipoles in an OLED-like layer stack (Fig. 1b).[25–27]

This method allows for the determination of the energy distribution to the different optical modes as well as the influence of the Purcell effect. The device archictecture we used consists of 150 nm of ITO on glass, 30 nm of the hole-injection material PEDOT:PSS, an optimized thickness of the hole transport layer NPB, 5 nm of LHP NCs as emission layer, 10 nm of OXD-7 as hole blocker, an optimized thickness of Aluminium-tris(8-hydroxychinolin) (Alq$_3$) as electron transport layer, 10 nm Ca and 100 nm Al. The optimized thickness values can be found in the supporting information. From the simulations we extract the alignment constant (ζ) which can be split into contributions of φ_{TDM} and n_{EML} (Fig. 1c). The plot clearly shows how reducing φ_{TDM} or increasing n_{EML} leads to a higher outcoupling efficiency. Please note that the primary outcome of the numerical simulation is the alignment constant ζ, which contains all the information needed to calculate the light outcoupling efficiency of a given device stack. The refractive index itself is only needed in order to determine the TDM angle. Importantly, an uncertainty in the refractive index will not affect the analysis of the
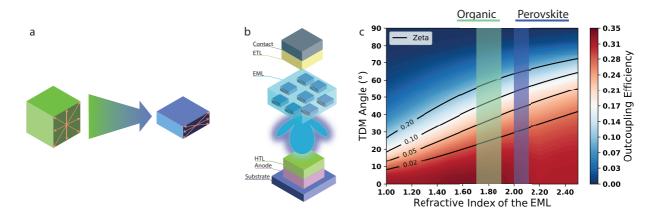
Figure 1: **Transition dipole moment and light outcoupling in perovskite nanocrystal LEDs.** **a)** Schematic of the possible orientations of the TDM in perovskite nanocrystals. While isotropic in nanocubes, the angle is strongly restricted in the vertical direction for thin nanoplatelets. **b)** Depiction of an exemplary stack design used to simulate the outcoupling efficiency of perovskite LEDs. HTL, EML and ETL denote hole transport layer, emission layer and electron transport layer, respectively. **c)** The outcoupling efficiency in dependence of the angle of the emissive TDM and the refractive index of the EML. Both quantities can be combined to the alignment constant (ζ). Samples with the same ζ value yield identical light outcoupling efficiency, as indicated by the contour lines.

efficiency.

In case of LHP NCs, the value of n_{EML} deserves some comment. The Bruggemann approach is typically used to obtain an effective refractive index and taking into account the high value of the inorganic perovskite layer and the lower value of the organic ligands, one can assume a value of $n_{EML} = 2.0$ for LHP NCs.[28] Clearly, the perovskites have a significant advantage in this case in comparison to traditional organic emitters, as they possess a relatively high refractive index. Concerning the angle φ_{TDM}, CsPbBr$_3$ perovskite nanocubes are only weakly confined and thus do not exhibit a preferential orientation for the TDM (see Fig. 1a). This reduces their overall efficiency of outcoupling with respect to the best organic emitters. However, as the thickness of the NCs is reduced to obtain NPls, the angle of the TDM becomes progressively restricted in its orientation, which is in the plane of the NPl. This can be exploited if the NPls are arranged to lie flat on the device stack, as the radiation is emitted perpendicular to the TDM, and so would be focused out of the LED. Note that this consideration is only valid for thin emissive layers which merely act as

6

the source of radiation but are too thin to directly contribute to wave propagation.[20]

2.2 Radiation pattern analysis

CsPbBr$_3$ NPls with a controllable thickness from 1.2 to 3.6 nm, corresponding to two to six monolayers (MLs), were obtained following a previously described reprecipitation method (see SI for further details).[18] To measure the optical properties of the NCs in detail, we spin-coated the dispersions (in toluene) onto glass substrates, yielding nearly closed monolayers of NCs. The narrow thickness leads to a pronounced quantum confinement, which results in a strong blueshift of the photoluminescence emission with decreasing thickness. Narrow, single emission peaks are observed for thin films of these samples varying from 432 nm for the 2 ML sample to 497 nm for the 6 ML sample, as shown in the Supporting Information (cf. Figure S1). The perovskite nanocrystals exhibit narrow emission spectra and emission maxima in the blue part of the optical spectrum, resulting in improved color coordinates compared with traditional blue organic emitters, as depicted in Fig. 2a.

Angular dependent radiation patterns were taken using the experimental setup shown in Fig. 2b. Therein, the sample is placed on top of a spherical prism and excited with a 375 nm cw laser diode. The PL signal passes through the prism and is collected by a spectrometer (Princeton Instruments Acton 2300i with Princeton Instruments PyLoN detector). Angle-dependent emission spectra are acquired by rotating the sample with respect to the detection optics. These spectra can be modelled according to a procedure described in literature.[24,28,31,32] In short, the angular dependent light emission from the layer stack is simulated using a classical dipole model. Therein, each of the three orthogonal dipole orientations x, y and z (with x & y lying in the substrate plane (horizontal) and z being perpendicular to it (vertical)) are treated separately, because they each contribute in a characteristic manner to the radiation output. Since the angular dependent radiation pattern is measured under transverse magnetic polarization (see Fig. 2b) only the x- and z-components are relevant here. Their relative contributions to the measured signal are determined by numerical fit-
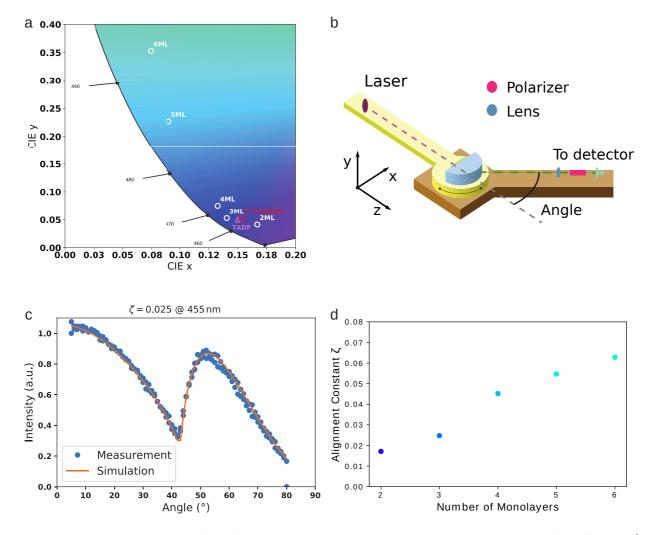
Figure 2: **Determining the alignment constant ζ in perovskite nanoplatelets. a)** CIE1931 color coordinates for $CsPbBr_3$ nanoplatelets compared to state-of-the-art organic emitters.[29,30] **b)** Illustration of the angular dependent spectroscopy setup. Angular dependent radiation patterns are obtained via rotation of the sample with respect to the detector. **c)** Angular dependent radiation pattern of a 3 ML sample (blue dots) and the simulated pattern (orange line). The simulation is used to obtain the alignment constant ζ. **d)** ζ values for nanoplatelets of thickness between 2ML and 6ML.

ting, yielding the alignment constant ζ. For the calculation of the total (angle integrated) light emission and the concomitant device light outcoupling efficiency, the y-component is then used identical to x, as the thin films have no preferred alignment within the substrate plane.

A representative spectrum is plotted in Fig. 2c for 3 ML platelets (blue dots). The result for this case is plotted in orange, yielding an extremely good fit to the data. From this

fit we can extract the value of the alignment constant, in this case we obtain $\zeta = 0.025$. This and all following values for ζ were extracted at the peak wavelength of the respective spectrum. Individual fits for each of the platelet thicknesses can be found in the Supporting Information (Figure S2).

Measurements of the alignment constant ζ were performed for each of the different CsPbBr$_3$ platelet thicknesses. The thickest NPls with 6 ML exhibit a ζ value of 0.062, which is slightly lower than the value obtained for CsPbBr$_3$ nanocubes in a previous publication.[24] As the thickness of the NPls decreases, the value of ζ also decreases down to only 0.025 for the 3ML and 0.018 for the 2ML NPls (Fig. 2d). The value for the 3ML NPls is only slightly higher than that previously observed for NPls of the same thickness.[28] However, in this previous publication, the NPls were covered with a thin layer of Al$_2$O$_3$, which significantly reduces the ζ value.

3 Efficiency analysis

Decreasing the alignment constant leads to an increase in the outcoupling efficiency of the PeLED. This benefit is mostly caused by a decrease in surface plasmon polariton coupling, which is inversely correlated to the TDM angle to the substrate. Hence, the energy outcoupled into free space increases as ζ is lowered. This is shown in Fig. 3a, where the outcoupling efficiency is plotted in dependence of the TDM angle and the refractive index of the EML. Here, we have added the values not only for all of the measured NPls, but also for some prototypical organic emitters. The benefit of the enhanced refractive index of the perovskites is clearly visible. This is mainly due to the refractive index contrast between the EML and the organic semiconductor transport layers ($n_{\mathrm{EML}} > n_{\mathrm{org}}$).[20] Again, please note that the light outcoupling efficiency is primarily given by the value of the alignment constant indicated as contour lines in Fig. 3a. Moreover, these values would not change even if the effective refractive index of the NPl layer were slightly thickness dependent.
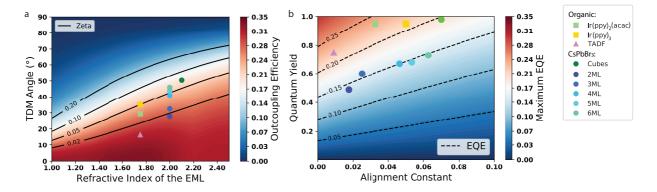
Figure 3: **Outcoupling efficiency and EQE limits of PeLEDs. a)** The outcoupling efficiency for perovskite nanocrystals and some prototypical organic emitters[29,33] in dependence on the TDM angle and the refractive index of the EML. The values of ζ decrease for decreasing nanoplatelet thickness and, consequently, light outcoupling increases. **b)** Performance of the investigated exemplary PeLED stack for different quantum yields and alignment constants of the emissive nanocrystals. The colored dots indicate the EQE limit of different $CsPbBr_3$ nanocrystal shapes. While nanocubes are close to their theoretical maximum of about 20 %, device performance for the different nanoplatelets could be enhanced by increasing the quantum yield of the emissive perovskite. Note that PLQY values were taken from literature.[18]

The oucoupling directly affects the efficiency of the overall device, as depicted in Fig. 3b. For $CsPbBr_3$ nanocubes, with a quantum yield approaching unity, the alignment constant value of 0.07 limits the maximum device efficiency (EQE) to 20%.[24] In contrast, the NPls have alignment constants that are significantly lower (down to 0.018 for 2ML NPls). Consequently, their light outcoupling efficiencies are all higher than that of the nanocubes, reaching 28 % for the thinnest sample. However, currently, all of the NPl LEDs show very similar performance with EQEs of about 15 %, which is clearly less than the 20 % for nanocubes, because the potentially higher outcoupling is compensated by a reduced PLQY of the material.[18] Thus, two direct strategies for improving the EQE are obvious. First, by improving the quantum yield of the NPls through optimized syntheses and, second, through encapsulation of the EML in a thin layer of high refractive index material, as previously demonstrated.[28]

Interestingly, in comparison to state-of-the-art devices found in literature,[15,34] their efficiencies significantly lag behind the theoretical predictions presented here. Blue PeLEDs containing NPls currently reach only 0.3 % and 0.55 % for three and five ML of $CsPbBr_3$,

respectively. While the devices exhibit narrow color-pure emission and reasonable stability during device operation, the limiting factor is currently not the performance of the emitter or the out-coupling. Instead the deep valence band position of blue LHP NPls constitutes an energetic barrier for hole injection, leading to enhanced nonradiative recombination at the perovskite-transport layer interface.

4   Conclusions

In summary, we have investigated the effect of the orientation of the transition dipole moment of perovskite nanoplatelets on the outcoupling efficiency and consequently the maximum efficiency achievable for PeLEDs. Using the alignment constant (ζ), which factors in not only the TDM angle but also the refractive index of the EML, we find a strong decrease in ζ values with decreasing thickness of the perovskite nanoplatelets. This is due to the progressive confinement of excitons within the NPls, which leads to a stronger orientation of the TDM and a concomitant blue-shifted emission. Estimations reveal a performance limit of 20 % for weakly confined green-emitting nanocubes due to their nearly vertical alignment of the emissive TDM. While for the blue-emitting nanoplatelets the alignment constant can be strongly reduced, they also exhibit reduced PLQY, which more than cancel out the increased outcoupling efficiency. The EQE is thus currently limited to approximately 15 %. However, by increasing the quantum yield of the thin quantum confined nanoplatelets to the value of the nanocubes, the EQE could be boosted to almost 30 %. In current state-of-the-art devices for deep-blue emitting $CsPbBr_3$ nanocrystals, which only reach about 0.3 % EQE the most limiting factor, however, is the difficulty in injecting charges efficiently, an issue which needs to be solved in order to come closer to the theoretical limits.

Acknowledgments

References

(1) Brenner, T. M.; Egger, D. A.; Kronik, L.; Hodes, G.; Cahen, D. Hybrid organic—inorganic perovskites: low-cost semiconductors with intriguing charge-transport properties. *Nature Reviews Materials* **2016**, *1*, 15007.

(2) Egger, D. A.; Bera, A.; Cahen, D.; Hodes, G.; Kirchartz, T.; Kronik, L.; Lovrincic, R.; Rappe, A. M.; Reichman, D. R.; Yaffe, O. What Remains Unexplained about the Properties of Halide Perovskites? *Advanced materials (Deerfield Beach, Fla.)* **2018**, *30*, e1800691.

(3) Yablonovitch, E. SOLAR CELLS. Lead halides join the top optoelectronic league. *Science (New York, N.Y.)* **2016**, *351*, 1401.

(4) Brittman, S.; Luo, J. A Promising Beginning for Perovskite Nanocrystals: A Nano Letters Virtual Issue. *Nano letters* **2018**, *18*, 2747–2750.

(5) Kovalenko, M. V.; Protesescu, L.; Bodnarchuk, M. I. Properties and potential optoelectronic applications of lead halide perovskite nanocrystals. *Science (New York, N.Y.)* **2017**, *358*, 745–750.

(6) Sutherland, B. R.; Sargent, E. H. Perovskite photonic sources. *Nature Photonics* **2016**, *10*, 295.

(7) Tan, Z.-K.; Moghaddam, R. S.; Lai, M. L.; Docampo, P.; Higler, R.; Deschler, F.; Price, M.; Sadhanala, A.; Pazos, L. M.; Credgington, D.; Hanusch, F.; Bein, T.; Snaith, H. J.; Friend, R. H. Bright light-emitting diodes based on organometal halide perovskite. *Nature Nanotechnology* **2014**, *9*, 687.

(8) Lin, K. et al. Perovskite light-emitting diodes with external quantum efficiency exceeding 20 per cent. *Nature* **2018**, *562*, 245.

(9) Zou, W. et al. Minimising efficiency roll-off in high-brightness perovskite light-emitting diodes. *Nature Communications 9*, 608.

(10) Li, G.; Huang, J.; Zhu, H.; Li, Y.; Tang, J.-X.; Jiang, Y. Surface Ligand Engineering for Near-Unity Quantum Yield Inorganic Halide Perovskite QDs and High-Performance QLEDs. *Chemistry of Materials* **2018**, *30*, 6099–6107.

(11) Xu, W. et al. Rational molecular passivation for high-performance perovskite light-emitting diodes. *Nature Photonics* **2019**, *13*, 418.

(12) Zhao, X.; Ng, J. D. A.; Friend, R. H.; Tan, Z.-K. Opportunities and Challenges in Perovskite Light-Emitting Devices. *ACS Photonics* **2018**, *5*, 3866–3875.

(13) Levchuk, I.; Osvet, A.; Tang, X.; Brandl, M.; Perea, J. D.; Hoegl, F.; Matt, G. J.; Hock, R.; Batentschuk, M.; Brabec, C. J. Brightly Luminescent and Color-Tunable

Formamidinium Lead Halide Perovskite FAPbX3 (X = Cl, Br, I) Colloidal Nanocrystals. *Nano letters* **2017**, *17*, 2765–2770.

(14) Lignos, I.; Protesescu, L.; Emiroglu, D. B.; Maceiczyk, R.; Schneider, S.; Kovalenko, M. V.; deMello, A. J. Unveiling the Shape Evolution and Halide-Ion-Segregation in Blue-Emitting Formamidinium Lead Halide Perovskite Nanocrystals Using an Automated Microfluidic Platform. *Nano letters* **2018**, *18*, 1246–1252.

(15) Hoye, R. L. Z.; Lai, M.-L.; Anaya, M.; Tong, Y.; Gałkowski, K.; Doherty, T.; Li, W.; Huq, T. N.; Mackowski, S.; Polavarapu, L.; Feldmann, J.; MacManus-Driscoll, J. L.; Friend, R. H.; Urban, A. S.; Stranks, S. D. Identifying and Reducing Interfacial Losses to Enhance Color-Pure Electroluminescence in Blue-Emitting Perovskite Nanoplatelet Light-Emitting Diodes. *ACS energy letters* **2019**, *4*, 1181–1188.

(16) Gangishetty, M. K.; Hou, S.; Quan, Q.; Congreve, D. N. Reducing Architecture Limitations for Efficient Blue Perovskite Light-Emitting Diodes. *Advanced materials (Deerfield Beach, Fla.)* **2018**, *30*, e1706226.

(17) Ochsenbein, S. T.; Krieg, F.; Shynkarenko, Y.; Rainò, G.; Kovalenko, M. V. Engineering Color-Stable Blue Light-Emitting Diodes with Lead Halide Perovskite Nanocrystals. *ACS applied materials & interfaces* **2019**,

(18) Bohn, B. J.; Tong, Y.; Gramlich, M.; Lai, M. L.; Döblinger, M.; Wang, K.; Hoye, R. L. Z.; Müller-Buschbaum, P.; Stranks, S. D.; Urban, A. S.; Polavarapu, L.; Feldmann, J. Boosting Tunable Blue Luminescence of Halide Perovskite Nanoplatelets through Post-synthetic Surface Trap Repair. *Nano letters* **2018**, *18*, 5231–5238.

(19) brweb, BT.2020 : Parameter values for ultra-high definition television systems for production and international programme exchange. https://www.itu.int/rec/R-REC-BT.2020-2-201510-I/en.

(20) Shi, X.-B.; Liu, Y.; Yuan, Z.; Liu, X.-K.; Miao, Y.; Wang, J.; Lenk, S.; Reineke, S.; Gao, F. Optical Energy Losses in Organic-Inorganic Hybrid Perovskite Light-Emitting Diodes. *Advanced Optical Materials* **2018**, *6*, 1800667.

(21) Bradley, D. D. C.; Friend, R. H.; Holmes, A. B.; Tsutsui, T.; Aminaka, E.; Lin, C. P.; Kim, D.-U. Extended molecular design concept of molecular materials for electroluminescence: Sublimed–dye films, molecularly doped polymers and polymers with chromophores. *Philosophical Transactions of the Royal Society of London. Series A: Mathematical, Physical and Engineering Sciences* **1997**, *355*, 801–814.

(22) Becker, M. A. et al. Bright triplet excitons in caesium lead halide perovskites. *Nature* **2018**, *553*, 189.

(23) Tamarat, P.; Bodnarchuk, M. I.; Trebbia, J.-B.; Erni, R.; Kovalenko, M. V.; Even, J.; Lounis, B. The ground exciton state of formamidinium lead bromide perovskite nanocrystals is a singlet dark state. *Nature Materials* **2019**, *18*, 717.

(24) Jurow, M. J.; Lampe, T.; Penzo, E.; Kang, J.; Koc, M. A.; Zechel, T.; Nett, Z.; Brady, M.; Wang, L.-W.; Alivisatos, A. P.; Cabrini, S.; Brütting, W.; Liu, Y. Tunable Anisotropic Photon Emission from Self-Organized CsPbBr3 Perovskite Nanocrystals. *Nano letters* **2017**, *17*, 4534–4540.

(25) Brütting, W.; Frischeisen, J.; Schmidt, T. D.; Scholz, B. J.; Mayr, C. Device efficiency of organic light-emitting diodes: Progress by improved light outcoupling. *physica status solidi (a)* **2013**, *210*, 44–65.

(26) Barnes, W. L. Fluorescence near interfaces: The role of photonic mode density. *Journal of Modern Optics* **2009**, *45*, 661–699.

(27) Penninck, L.; de Visschere, P.; Beeckman, J.; Neyts, K. Dipole radiation within one-dimensional anisotropic microcavities: A simulation method. *Optics express* **2011**, *19*, 18558–18576.

(28) Jurow, M. J.; Morgenstern, T.; Eisler, C.; Kang, J.; Penzo, E.; Do, M.; Engelmayer, M.; Osowiecki, W. T.; Bekenstein, Y.; Tassone, C.; Wang, L.-W.; Alivisatos, A. P.; Brütting, W.; Liu, Y. Manipulating the Transition Dipole Moment of CsPbBr3 Perovskite Nanocrystals for Superior Optical Properties. *Nano letters* **2019**, *19*, 2489–2496.

(29) Chan, C.-Y.; Cui, L.-S.; Kim, J. U.; Nakanotani, H.; Adachi, C. Rational Molecular Design for Deep–Blue Thermally Activated Delayed Fluorescence Emitters. *Advanced Functional Materials* **2018**, *28*, 1706023.

(30) Pal, A. K.; Krotkus, S.; Fontani, M.; Mackenzie, C. F. R.; Cordes, D. B.; Slawin, A. M. Z.; Samuel, I. D. W.; Zysman-Colman, E. High-Efficiency Deep-Blue-Emitting Organic Light-Emitting Diodes Based on Iridium(III) Carbene Complexes. *Advanced materials (Deerfield Beach, Fla.)* **2018**, *30*, e1807138.

(31) Frischeisen, J.; Yokoyama, D.; Adachi, C.; Brütting, W. Determination of molecular dipole orientation in doped fluorescent organic thin films by photoluminescence measurements. *Applied Physics Letters* **2010**, *96*, 073302.

(32) Morgenstern, T.; Schmid, M.; Hofmann, A.; Bierling, M.; Jäger, L.; Brütting, W. Correlating Optical and Electrical Dipole Moments To Pinpoint Phosphorescent Dye Alignment in Organic Light-Emitting Diodes. *ACS applied materials & interfaces* **2018**, *10*, 31541–31551.

(33) Graf, A.; Liehm, P.; Murawski, C.; Hofmann, S.; Leo, K.; Gather, M. C. Correlating the transition dipole moment orientation of phosphorescent emitter molecules in OLEDs with basic material properties. *J. Mater. Chem. C* **2014**, *2*, 10298–10304.

(34) Yang, D.; Li, X.; Zeng, H. Surface Chemistry of All Inorganic Halide Perovskite Nanocrystals: Passivation Mechanism and Stability. *Advanced Materials Interfaces* **2018**, *5*, 1701662.